

# Considerations on the Effects that Core Material Machining has on an Electrical Machine's Performance

Ahmed Al-Timimy, *Member, IEEE*, Gaurang Vakil, Michele Degano, Paolo Giangrande, *Member, IEEE*, Chris Gerada, *Member, IEEE* and Michael Galea *Member, IEEE*

**Abstract**--An often-overlooked aspect during the development process of electrical machines, is the validity and accuracy of the machine material properties being used at the design stage. Designers usually consider the data provided by the materials supplier, which is measured on material in an unprocessed state. However, the fact that the machining processes required to produce the finished product (e.g. the stator core) can permanently vary the material properties is very often neglected. This paper therefore deals with and investigates the effects that such processes can have on the overall machine performance. To do this, three sets of material data, based on 1) the materials suppliers' data, 2) materials data based on conventional characterization methods and 3) materials data based on test samples that include the manufacturing processes, are used to develop three versions of the same baseline machine. The results of these three machines are then compared and the resulting variations of the machine's performance presented and described.

The chosen baseline machine is a high performance and relatively high speed, aerospace, electrical machine. Special attention is focused on the efficiency maps of the machine as this aspect is highly dependent on the material properties that are the most sensitive to manufacturing processes such as the material's anhysteretic BH curve and its specific core loss.

**Index Terms**--magnetic materials, manufacturing processes, performance analysis, permanent magnet motors.

## I. INTRODUCTION

**I**N the world of electrical machines, a very important design aspect is related to the properties and the characteristics of the machine materials, including those of the copper and the hard and soft magnetic materials. With these properties in hand, electrical machine designers have for decades developed their machines in accordance with their own design and analysis procedures. With recent advances in computational resources, finite element (FE) software packages and the advent of whole suites of new materials, these material properties are today becoming ever more important in the quest towards higher performance, higher speeds and higher efficiency machines.

Traditionally, machine designers perform their development by considering the data provided by the material suppliers. For example, the BH characteristics of the laminated material used for the stator and rotor cores will be usually made available by either the material supplier or the material distributor. These characteristics are usually imported into the designer's modeling tools with the assumption that the data provided by the manufacturer are accurate and representing exactly the material characteristic for the specific application.

However, it is important to note that such data are usually based on conventional testing and characterization methods. For example, in the case of soft magnetic materials, the data will be achieved from standard tests such as the Epstein frame test and the single sheet test [1, 2]. These conventional characterization methods achieve the data based on tests performed on representative test samples, such as a simple toroid or square-shaped cubes.

The reality however is that the machine designer is then using this data (obtained from simplistic test samples) to develop a much more complex geometry and shape, such as for example a stator core geometry. At this stage all is fine, but when one considers that to actually manufacture that stator core a process comprising several steps of manufacturing, e.g. electrical discharge machining (EDM) for cutting, welding, stamping etc... is required, then the question relative to the validity of the original data arises.

It is well known [3–13] that these manufacturing processes all have a significant and permanent effect on the magnetic properties of the material, especially on the BH curve and the specific core loss properties of the material. This implies that the materials being used for the actual machine no longer reflect the material properties given by their original data sheets. If these variations are not taken into account by the machine designer, then these can have a significant effect in terms of the general performance characteristics of any prototyped machine.

Usually discrepancies between the expected and the measured results, resulting from these effects are simply waived off and lumped with the "manufacturing error". However, it is also true that these discrepancies and variations do have an effect on the performance characteristics of the machine [14] Today there is an ever-increasing need for higher performances and cost requirements (e.g. highly

---

A. Al-Timimy, G. Vakil, M. Degano, P. Giangrande, M. Galea and C. Gerada are with the Power Electronics, Machines and Control Group, University of Nottingham, Nottingham, UK (e-mail: Ahmed.Al-Timimy@nottingham.ac.uk).

M. Degano, M. Galea and C. Gerada are also with the University of Nottingham Ningbo China, Ningbo, China.

demanding application areas such as for aerospace and automotive applications). In such cases the electrical machine is typically already pushed to the technological boundaries represented by the thermal and magnetic limits [15–17]. Thus, to achieve the required specifications, even the smallest discrepancy and/or variation needs to be taken into account. For this reason, it is necessary to determine the effects on electrical machines' performance, due to changes and variations in the magnetic properties of the material resulting from manufacturing processes.

The main aim of this paper is thus to investigate the aforementioned manufacturing effects on electrical machine design and their overall performance. As vessel to investigate these effects, a previously developed 9-slot/8-pole, permanent magnet synchronous motor (PMSM) [18, 19] for an aerospace pump application is considered. In order to do this, three main data sets (DS) of material properties are used, namely

DS1 - The data provided by the material supplier for the laminated sheet steel (as provided in the data sheet).

DS2 - The data of the same material characterized in house, using standard, conventional test samples.

DS3 - The data of the same material characterized in house, using test samples, composed of completely manufactured stator core geometries (i.e. that include all the manufacturing processes).

For DS2 and DS3 above, the data is captured on a purposely-built, magnetic material characterization set-up as introduced later in Section III.

A major objective of this work is to accurately map the machine's efficiency ratings at different operating points, while of course taking into account the influence of manufacturing process on the magnetic properties of the hard magnetic material. For the machine in question, the stator core is made from Cobalt Iron (CoFe) laminated material.

## II. MATERIAL AND MANUFACTURING EFFECTS ON MACHINE DESIGN

In literature, the variations in the material properties and core loss due to the manufacturing process on the stator core are investigated in [3–13]. However, there is a very small amount of literature that considers the effect of machining processes on the actual machine performance. In [8], the influence of material degradation on the performance of PM machine due to cutting has been studied. In this work, a single sheet lamination, with different amount of cuts, has been used for evaluating the magnetic properties which then is used to determine the operating behaviour of the PM machine. In [9], the authors investigate the effect of 6.5% Silicon Steel (SiFe) and CoFe alloy materials on machine performance where the application is quite high speed and therefore material properties play even a bigger role. The magnetic material properties are experimentally characterized by using a conventional single sheet tester in order to obtain the anhysteretic BH curves and the specific core loss. However, the influence of the manufacturing process on the machine performance is not considered. In another works, the performance of a small power induction motors has been

investigated using a suite of different magnetic materials, such as M600-50A, NO20, NO12 and amorphous steel alloy 2605sA1, for the stator core [10, 11]. The anhysteretic BH curves and the specific core loss have been obtained using a toroidal sample and the induction motor performance has been evaluated in the speed range from 0 to 3000 rpm at full load condition. The effect of welding processes is investigated in [12], with focus on the influence of welding on the material losses. Experimental results using a ring core at different frequencies and flux densities are presented. The results show an increase of the core loss by 10% due to the welding process, while the effect on the machine efficiency is about 0.11%. The welding effect on small slot-less PMSM performance has been also studied in [13]. Stator cores made of SiFe and nickel iron steel sheets are experimentally characterised to investigate the changes in magnetic material properties. A main outcome of the study is that negligible influence on both the induced back-EMF and output torque was found, while an increase of core loss from 32% to 44% was observed. This is due to the deterioration of the material properties in the area of the welding seams. Since, the welding seams partly destroy the sheet insulation layer.

All the above indicates that while a number of previous works do acknowledge and study the effects that manufacturing processes have on the material itself, however only a couple of cases actually further the analysis into the domain of the machine performance.

## III. THE BASELINE MACHINE

Based on the design requirements and constraints presented in previous works [18] and [19], an 8-pole/9-slot PMSM has been designed and optimized. In [20] the thermal management for the designed PMSM has been investigated in detail. Originally the machine was developed with a SiFe material. However, for high power to mass and high power to volume ratios applications such as for the aerospace application considered in this study, the overall performance advantages associated with a high saturation flux density material such as CoFe can usually overcome the related disadvantages that include a higher material price, availability on market and mass density (8120 kg/m<sup>3</sup> compared to 7650 kg/m<sup>3</sup> for SiFe material) [21]. Due to this, the machine was then re-developed with a CoFe stator core.

CoFe lamination sheets are characterized by lower mechanical strength and higher sensitivity to magnetic property degradation due to induced stresses in the cutting and punching process [21, 22]. Therefore, one or more annealing cycles, during the manufacturing stage, are necessary to restore the optimum magnetic properties [3, 22, 23]. Since the stator requires several machining processes then its magnetic properties, such as the magnetization BH curve and the specific core loss, will change and this requires particular attention.

Fig. 1 shows the torque-speed characteristics of the application. A maximum continuous torque ( $T_{rated}$ ) is required over a speed range from 0 to 8700 rpm. Beyond the

base speed ( $N_{base}$ ) of 8700 rpm, flux weakening is required until the maximum speed ( $N_{max}$ ) of 19000 rpm.

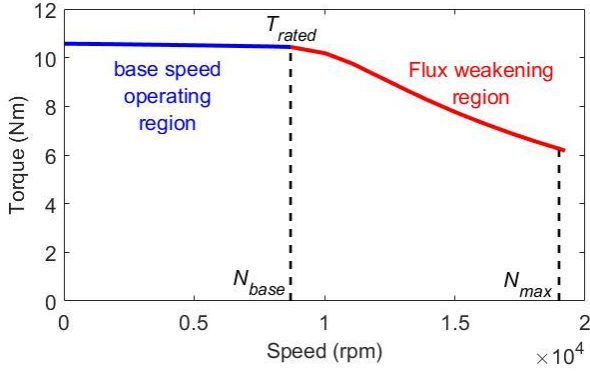


Fig. 1. Required torque-speed characteristic

Table I reports some of the main specifications and performance characteristics of the machine. It is important to note that these results are obtained when considering the original material data from the supplier, which in this paper is called DS1.

TABLE I  
Geometrical Dimensions and Performance Indicators

| Parameters                       | 10.5 Nm @<br>8700rpm | 5 Nm @<br>19000 rpm |
|----------------------------------|----------------------|---------------------|
| DC link voltage (V)              |                      | 270                 |
| Rated current (A)                |                      | 85                  |
| Stator outer diameter (mm)       |                      | 70                  |
| Split ratio                      |                      | 0.535               |
| Stack length (mm)                |                      | 80                  |
| Current density $J$ ( $A/mm^2$ ) |                      | 27.2                |

#### IV. CHARACTERIZATION OF MAGNETIC MATERIAL PROPERTIES

Different methods can be employed to investigate the magnetic properties and the core loss for the laminated material [24, 25]. As mentioned above, the most commonly used methods for measuring the magnetic properties of a laminated sheet are the Epstein frame test and the single sheet test. These testing methods are usually preferred due to their accuracy and simplicity [24, 25]. However, these methodologies are usually performed on representative test samples, such as a simple toroid or square-shaped cubes, where any effects of machining are only limited to the outer perimeter of the sample.

When the actual stator core shape and geometry is considered, the degradation effect of machining is higher as now the length of the “edges” of the sample that have seen machining is much longer. This can be appreciated by a visual comparison of Fig. 2 and Fig. 3, where it can be observed that the square sample of Fig. 2 is much less impacted by machining than the actual core geometry of Fig. 3. All this indicates that for a standard test sample, the measured BH curve and the specific core loss do not accurately represent the properties of the actual manufactured stator core of the

machine. This indicates that much more relevant and accurate material characteristics could be achieved from the actual machine stator core itself [25]. By using the actual stator core for material characterization, the effects of manufacturing processes, such as punching or cutting, stacking, welding and annealing, which might have a significant influence on the magnetic properties of the material [26], can be taken into account and fed back into the machine design process.

As explained in Section I, three different sets of material data are considered in this work. The data produced in-house (DS2 and DS3 in Section I) is achieved by using two different methods to evaluate the magnetic material properties. For DS2, i.e. data achieved on simplistic test samples, a single sheet of the lamination material is used. Fig. 2 (a) shows the sample of lamination sheet used for the test, while testing setup for this is shown in Fig. 2 (b). For DS3, i.e. with data achieved from a completely manufactured stator core, the test sample is shown in Fig. 3.

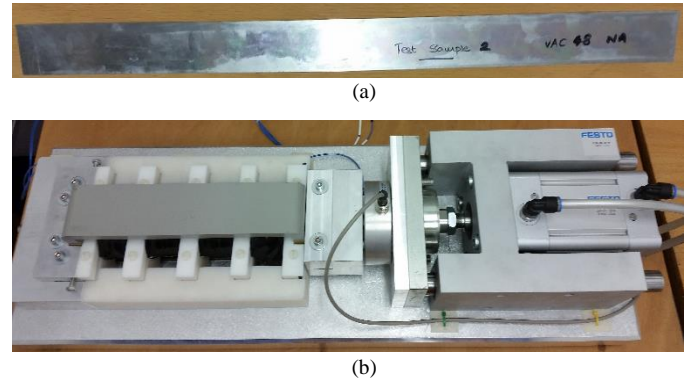


Fig. 2. Prepared material sample for testing: (a) Sheet sample. (b) Single sheet tester

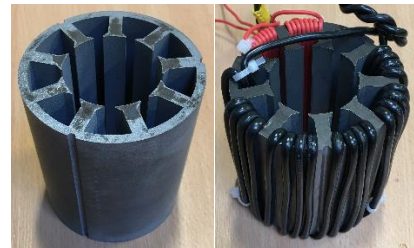


Fig. 3. CoFe material stator core (left) and wound stator core under test (right)

Both the stator core and lamination sheet used for the experiment are made from a CoFe alloy with 0.1mm lamination thickness. The CoFe sheets are made of approximately 49% cobalt, 49% iron and 2% Vanadium [21, 22]. Table II gives an overview of the CoFe material properties that were obtained from the manufacturer’s datasheet.

TABLE II  
Material Properties of the Investigated CoFe Stator Core Sample

| Lamination Thickness | Density       | Electrical Resistivity | Package Density | Saturation Flux Density |
|----------------------|---------------|------------------------|-----------------|-------------------------|
| 0.1 mm               | 8120 $kg/m^3$ | 0.4 $\mu\Omega m$      | 98%             | 2.3 T                   |

In order to accurately characterise these samples, a state of the art [9] testing facility that is available in-house was used to characterize these samples. Table III presents the specifications of the measuring system which is presented more in detail in [9, 27]. The core loss tests and BH magnetization curves at high frequency and high flux density for the slotted stator core and for the lamination sheet are performed under pure sinusoidal wave excitation.

TABLE III  
Specifications and Capabilities for the Measurement System

| Parameter                         | Quantity                      |                                  |
|-----------------------------------|-------------------------------|----------------------------------|
| Fundamental Frequency             | 2 – 100 kHz                   |                                  |
| Low Frequency Amplifier Capacity  | 100V 52 A (Peak)              |                                  |
|                                   | 60V 40A (Continuous)          |                                  |
| High Frequency Amplifier Capacity | 50V 10A (Peak and continuous) |                                  |
|                                   | Operating Temperatures        | Soft Magnetic Materials          |
|                                   | Hard Magnetic Materials       | -40°C to 300°C                   |
| Operating Stresses                | Soft Magnetic Materials       | 0 – 3 kN (Compression / Tension) |
|                                   | Hard Magnetic Materials       | 0 – 1kN (Compression)            |
| Excitation Waveforms              | Sine Wave                     |                                  |
|                                   | DC / Anhysteretic             |                                  |
|                                   | PWM                           |                                  |
|                                   | Harmonic                      |                                  |

#### A. Investigated samples

For the single sheet test, the investigated sample is a standard geometry with dimensions of 400 mm × 30 mm × 0.1 mm and magnetically characterized according to the specifications of the IEC 60404 standard. The lamination sheet is placed within two coils (primary and secondary) as shown in Fig. 2 (b) and the magnetic circuit is completed by two laminated C cores with ideally zero losses and zero MMF drop. The power core loss is then measured by subtracting the resistive drop from the input power.

For the stator core sample, the core is setup with two set of coils as shown in Fig. 3. The black coil is used as the primary circuit (excitation) and the red coil is used as the secondary circuit (measurement). The primary and the secondary number of turns are selected to be 21 and 10, respectively.

#### B. Magnetic measurements

For the magnetic material properties investigation, the slotted stator core and the lamination sheet are exposed to a defined magnetic field, in which the required primary excitation current is supplied by the high power amplifier and the maximum value of the magnetic field strength can be computed using (1), where  $N_1$  is the number of turns of the primary coil,  $i_1$  is the primary current and  $L_{-core}$  is the mean length of the magnetic flux path.

$$H(t) = \frac{N_1 \cdot i_1}{L_{-core}} \quad (1)$$

The induced voltage in the secondary coil is continuously recorded to determine the magnetic flux density as given by (2), where,  $N_2$  is the number of turns of the secondary coil and  $A_{-core}$  is the cross-sectional area of the sample.

$$B(t) = \frac{1}{N_2 A_{-core}} \int v_2 dt \quad (2)$$

For the stator core set-up, it is assumed that the flux leakage into the tooth area near to the back iron is negligible. In other words, it is assumed that all the flux crossing the core back iron is equal to the flux linkage to the primary winding. This assumption is verified in Section IV.

According to the assumption of negligible leakage flux the  $L_{-core}$  can be determined by  $L_{-core} = \pi * (R_{OD} + R_{ID})$ , where  $R_{OD}$  and  $R_{ID}$  are the outer and inner radius of the stator yoke. The cross-sectional area  $A_{-core}$  of the samples can be determined by (3), where  $M$  the total is mass of the stator yoke and  $\rho$  is the mass density of the material.

$$A_{-core} = \frac{M}{\rho * L_{-core}} \quad (3)$$

Finally, to determine the instantaneous value of the core loss, the current in the primary coil and the voltage of the secondary coil are measured simultaneously and multiplied by the coil ratio as given by (4),

$$P_{core} = \frac{N_1}{N_2} v_2 i_1 \quad (4)$$

The core loss density (W/kg) can be calculated using (5), where  $S_{bi}$  is the stator back-iron thickness.

$$P_{specific} = \frac{P_{core}}{\rho \cdot S_{bi} \cdot \pi \cdot (R_{OD}^2 - R_{ID}^2)} \quad (5)$$

## V. MEASUREMENT RESULTS

By post processing of the measured data according to the procedures explained in Section IV and using the geometrical specifications of the test samples, the required material properties, such as the BH magnetization curve, the DC relative permeability, the AC BH magnetizing curves and specific core loss can be determined [9].

#### A. Basic magnetic properties

First of all, the BH magnetization curve for both the slotted stator core (DS3) and the lamination sheet (DS2) are calculated. The obtained results are compared to the BH magnetization curve provided by the manufacturer (DS1), as shown in Fig. 4. Analysing the results of Fig 4, the BH curve as derived with data provided by the manufacturer shows higher relative permeability, which results in higher magnetic flux density.

The DC relative permeability for all the three different data scenarios is calculated and the results are shown in Fig. 5. It is clear that the relative permeability of the CoFe material is higher in the range of magnetic field strength 40 A/m to 100 A/m, while the relative permeability goes lower as the core material tends to saturate with higher magnetic field strength. Nevertheless, in the range from 1.5T to 2T, the relative permeability of the stator core is decreased by 67.5% and 47.6% compared to the slotted stator core data and lamination data respectively. However, the mismatch among the relative permeability values is negligible for magnetic field strength higher than 600 A/m.

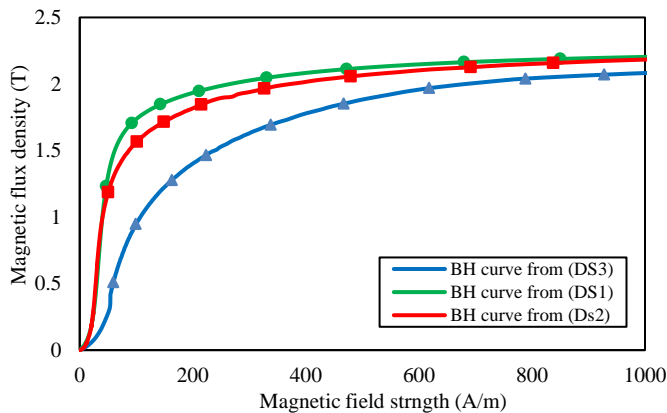


Fig. 4 Comparison among BH magnetization curves

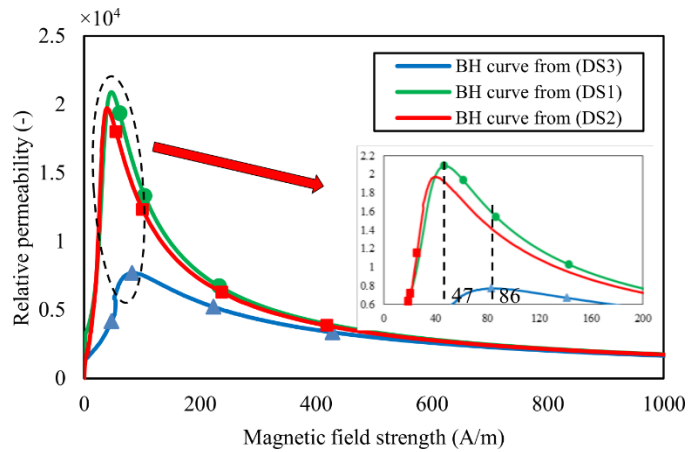


Fig. 5. Comparison among DC relative permeability

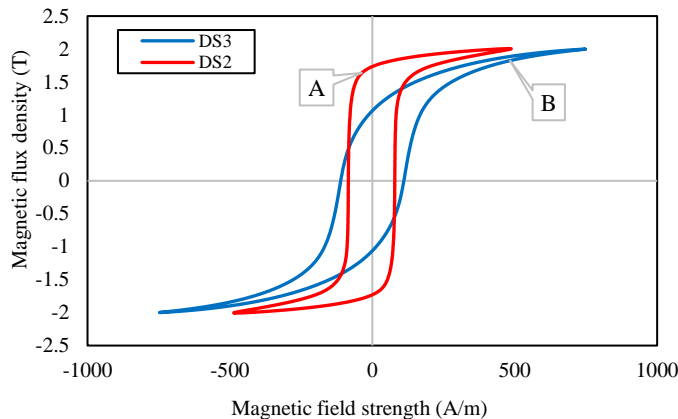


Fig. 6. AC hysteresis loop at 2 T and 1000 Hz

This indicates that the process using the data derived from the DS3 process results in a 50.3% difference in terms of stator flux density when compared to the other methodologies and thus already highlights the significant change that the manufacturing processes can inflict upon the stator material.

### B. Core losses

As the shape and size of the BH curve (hysteresis loop) depends on the frequency and the field intensity [28]. For the same flux density, the area of the AC hysteresis loop which represents the energy loss per cycle is higher with an increase of frequency and therefore, higher core loss per unit volume. To investigate the variation in the hysteresis loop, and hence variation in specific core loss, another AC test is carried out on the stator core and the lamination sheet with a flux density peak value of 2 T and frequency of 1000 Hz. The results are shown in Fig. 6. The increase of the hysteresis loop area is more visible in the case of the slotted stator core. In ideal condition, the BH curve should be as that shown in (Label A Fig. 6). However, this only counts for the laminated sample which does not go through any manufacturing process (only machining process). The actual stator core was manufactured by gluing the laminations together under pressure and then machining using EDM. The surface is heat treated while machining and the grain size is affected by stacking pressure.

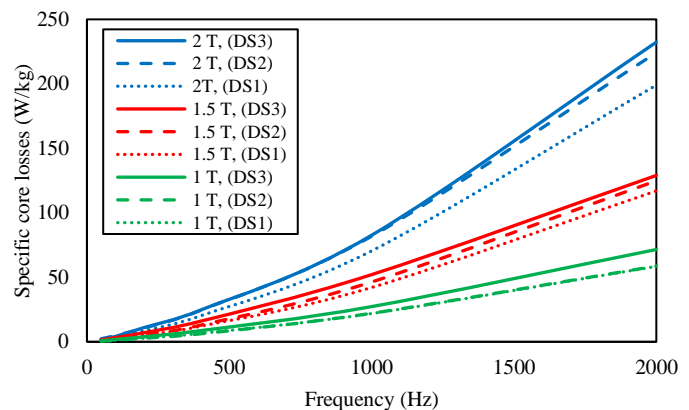


Fig. 7. Specific core loss comparisons utilizing the three DSs

Thus, the manufacturing process affects the performance of material (Label B Fig. 6), bringing the permeability down for the same magnetic field strength [13]. Also, there is a negligible effect of machining on laminated sheet as the strip is significantly wider 30 mm compared to the stator back iron which is 3.5 mm [13]. After investigating the hysteresis loops, the specific core losses were also determined in order to quantify the influence of machining processes on them.

The specific core loss as a function of different frequencies and flux densities are shown in Fig. 7. It is found that the core losses are increased in the range of flux density from 1 to 2 T, and the increase in the core loss becomes higher for higher frequencies. The measurements were carried out on both the sheet lamination and slotted stator core samples. The measurements on the stator core showed an increase in the core losses and change in the anhysteretic BH curve and the relative permeability due to the manufacturing process. Even if the flux density is lower for stator core DS3 compared to DS1 and DS2 as shown in Fig. 4. The losses are higher for DS3 compared to DS1 and DS2 as shown in Fig. 7. This is due to fact that, the area of the hysteresis curves for the manufactured stator core DS3 have changed and become bigger because of the manufacturing issue as shown in Fig. 6 and this reflected in the iron losses measurements. Same thing happens with the eddy current losses as well, because the manufacturing process affects the material properties.

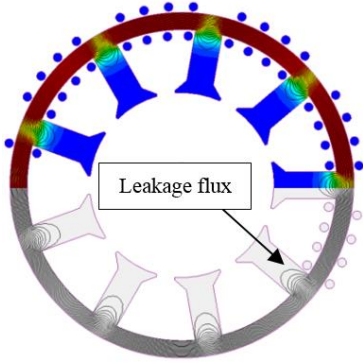


Fig. 8. Field flux lines in the stator core

TABLE IV

Comparison of the Back-EMF at No Load Condition for Different Data Sheets

|                      |           | DS1    | DS2    | DS3    |
|----------------------|-----------|--------|--------|--------|
| back-EMF<br>V (peak) | 4000 rpm  | 36.29  | 36.29  | 36.21  |
|                      | 8700 rpm  | 78.91  | 78.9   | 78.73  |
|                      | 13000 rpm | 117.89 | 117.88 | 117.62 |
|                      | 19000 rpm | 174.41 | 174.38 | 173.98 |

### C. Validating the negligible leakage assumption

In order to verify the assumptions made at the beginning of the analysis (negligible fringing flux inside the teeth), FE simulations on a slotted stator core, with the same geometrical dimensions and same number of turns as used in the experimental tests conducted on the manufactured stator, are carried out over a range of flux density levels. The results highlight a reduction in the flux density in the back iron of the slotted stator core due to the fringing flux into the teeth. Fig. 8 shows the magnetic flux lines in the stator core for a maximum current of 41A, where the flux density at the top of the teeth is reduced due to the flux fringing. By following the procedure presented in [3, 23], for different excitation currents, a correction factor has been introduced.

The corrected flux density in the stator core is then calculated considering the fringing factor and the results are shown in Fig. 9. As can be observed, the effect of the fringing flux on the BH curve is smaller than 5%. However, this has been considered in the computation of the motor performance.

## VI. THE INFLUENCE OF MATERIAL PROPERTIES ON MACHINE EFFICIENCY PERFORMANCE

Having identified and quantified the differences in the material properties that result from machining processes, it is then possible to use this information to assess the overall influence on the machine performance. In this section, the main consideration is done on the efficiency maps of the machine, which for this particular (relatively high speed) application are highly dependent on the specific core losses of the laminated material.

Traditionally, core loss in electrical machines is always severely underestimated [14]. By combining numerical simulations with the measured losses as explained above then more accurate representations of this important factor can be achieved

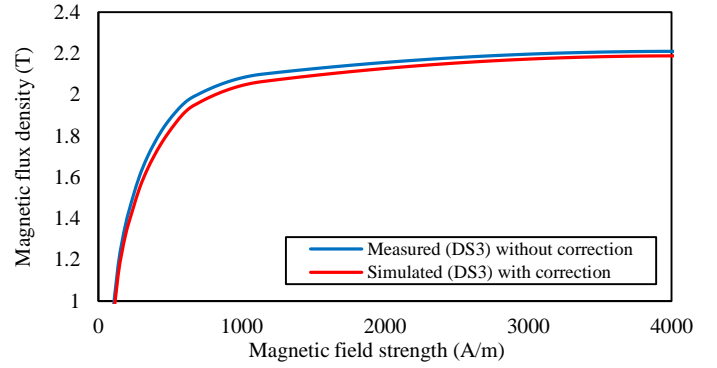


Fig. 9. BH magnetization curves for the measured stator core with and without correction

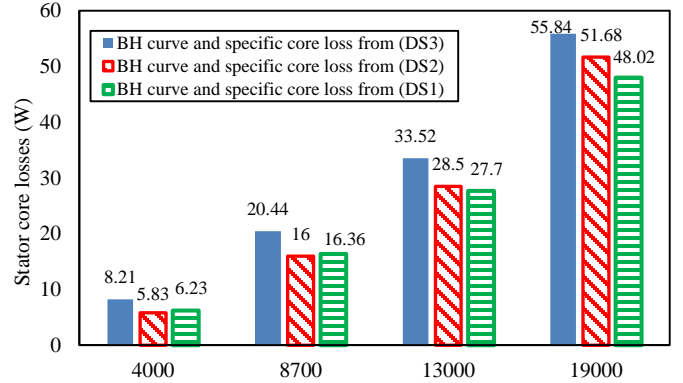


Fig. 10. No load stator core loss at different operating speeds

Also, this process permits the user to quantify the effect of the manufacturing process on the stator core loss increase for different machine operating conditions. To assess these effects, the machine is simulated with the three DSs of material data and the results compared for different operating conditions. Under no load condition, the maximum peak value of the back EMF at different operating speeds of 4000, 8700, 13000 and 19000 rpm are reported in Table IV. It can be seen that for different operating speeds the change in the no load voltage is negligible (<1%).

In Fig. 10 the core loss in the stator core at no load condition and for different operating speeds are presented. The results show that at low operating speed of 4000 rpm, the core loss using the measured data of the stator core is 1.98 W higher than the data provided by the manufacturer. As expected, the difference in the core loss increases towards the higher operating speeds of 19000 rpm with 16.28% difference between the measured data of stator core and data sheet of the manufacturer and 8% between the measured data of stator core and lamination.

To complete the machine characterization analysis, the performance under load conditions is also determined. By using the data from DS1, DS2 and DS3, the torque-speed curve is calculated for different operating speeds at rated torque condition. The results of machine performance at different operating points are presented in Fig. 11. In accordance with the simulation results presented in Fig. 11, a variation in the core loss and efficiency can be observed between the measured data and data sheet of the manufacturer.

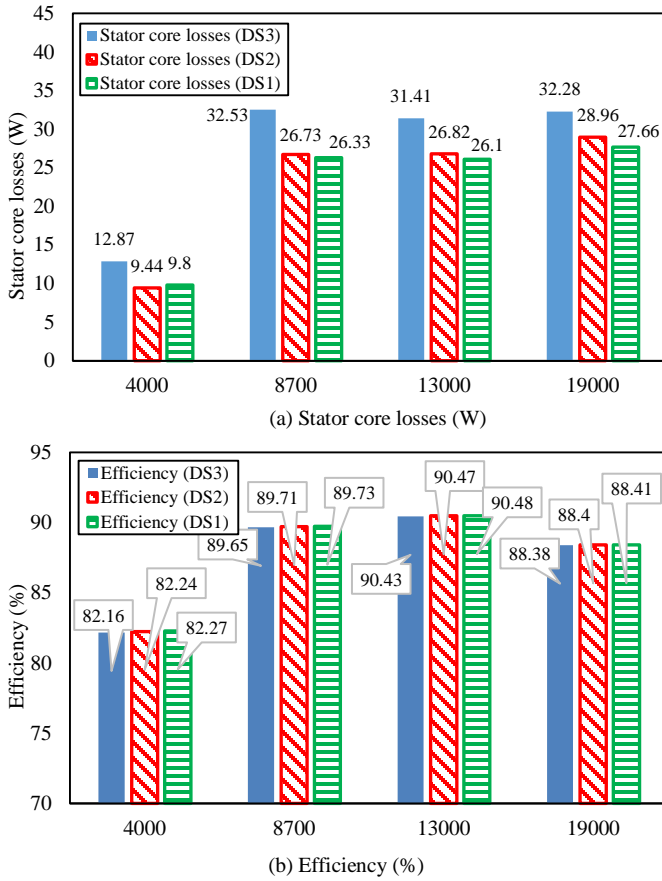


Fig. 11. Stator core loss and efficiency at rated torque condition and different operating speeds

This discrepancy is due to the deterioration of the magnetic material properties and the increased core loss as shown in Fig. 4 and Fig. 5.

In order to evaluate the effect of machining and manufacturing processes of the lamination sheet and stator core on the machine performance, different operational maps for the PMSM are described in detail. Fig. 12 shows the efficiency map calculated based on DS3 data, DS2 data and DS1 data respectively. The efficiency maps calculations are carried out over the entire speed and torque range and are including all the losses components (copper, stator core, permanent magnet, sleeve, rotor shaft and windage). It can be seen that the variation in efficiency increases towards lower operating points. Maximum reduction in efficiency is about 1% in Region A. This variation in efficiency is mainly caused by increased core loss and decrease in output torque. Figures 13 and 14 show the influence of the frequency and flux density on stator core loss and output torque, respectively. Fig. 13 shows the core loss in the operational map where  $C_{DS3}$ ,  $C_{DS2}$  and  $C_{DS1}$  are the core loss calculated as based on DS3, DS2 and DS1 respectively. It can be seen that results coming from FE simulation when the DS3 data is used, have the highest core loss because of the manufacturing processes on the stator core.

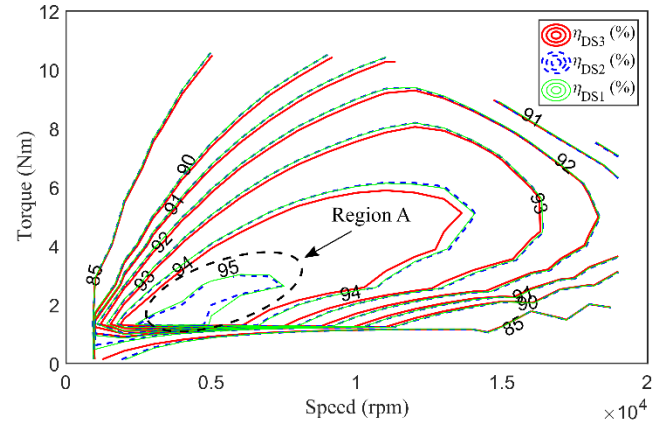


Fig. 12. Efficiency map of the PMSM

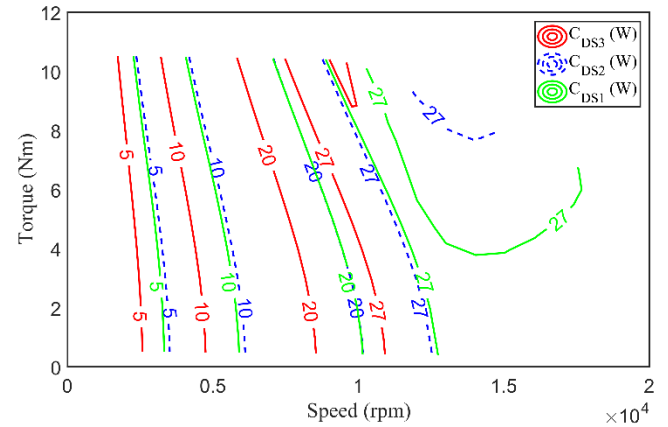


Fig. 13. Stator core losses map of the PMSM

At low rotational speeds and with different operating points, the variation in core loss is negligible (around 1 W) and its difference can increase up to 23% (rated operating point). These are caused by increased flux density and operating frequency at these operating points. While, within the area of the flux weakening between (9000 – 19000) rpm, the core loss increases until a certain operating point and then start to decrease due to the reduction of the flux density in the teeth and back iron. Also, it is found that the difference in core loss between  $C_{DS2}$  and  $C_{DS1}$  is not significant due to the small variation in the specific core loss obtained from the tested laminated sheet and manufacturer's datasheet values. This is true because no manufacturing processes were applied to achieve the DS2 data.

Fig. 14 shows the percentage of reduction in the output torque. This is given as  $(T_{DS3} - T_{DS2}) / T_{DS3}$  and as  $(T_{DS3} - T_{DS1}) / T_{DS3}$ , where  $T_{DS3}$ ,  $T_{DS2}$  and  $T_{DS1}$  are the output torque calculated based on DS3, DS2 and DS1 data, respectively. The influence of the manufacturing process on the slotted stator core is observed to be most dominant at lower magnetic field strength and tend to decrease towards the saturation region as shown in Fig. 4.

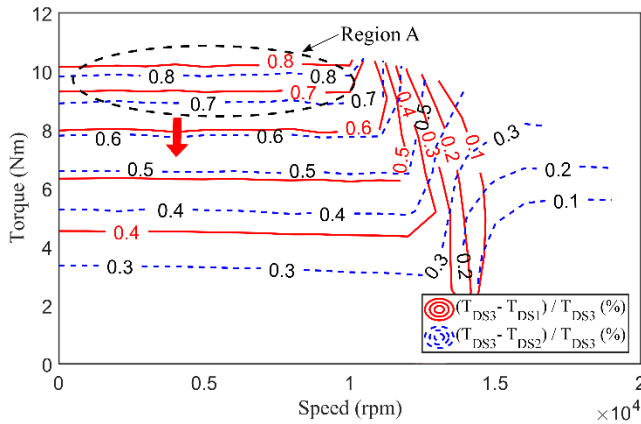


Fig. 14. Torque reduction map of the PMSM

This results in flux density reduction at lower magnetic field strength, leading to a lower output torque of the designed machine. The reduction in the output torque is noticeable in (Region A in Fig. 14) with high torque and low rotational speed. A maximum reduction of 0.8% in output torque was observed when experimental data from slotted stator core is used compared to manufacturers datasheet and lamination sheet values (Region A in Fig. 14). This reduction was caused due to the variation in the flux density (i.e. variation in anhysteretic BH curve) due to the different DSs. While, this variation in output torque was dropped to 0.3% at lower operating points. In particular, for the flux weakening region, it is important to note that the difference in the output torque decreases with the operating speed gradually increasing. Since, higher operating speeds required more negative d-axis current and therefore further reduction in the flux density and output torque.

## VII. CONCLUSION

In this paper, the effects that variations in material properties (due to manufacturing processes) can have on the general performance characteristics of electrical machines have been investigated and considered. In order to do this, an accurate characterization process that considers three different DSs was used in order to be able to compare how the overall machine performance is affected according to which DS, the machine designer chooses to use during his development and design of the machine. All existing sources in literature mainly limit themselves to highlighting the differences in the materials before and after specific, ‘standard’ machining processes. This paper however takes the analysis the full way and considers and compares the full machine performance in terms not only of material properties but also in terms of operational performance. The comparisons are done between the cases of 1) when ‘standard’ material properties are considered and 2) when ‘modified due to machining’ material properties are considered.

The investigation was done on a high performance and relatively high speed PMSM for an aerospace application. In

this work, special attention was focused on the efficiency maps of the machine as this aspect is highly dependent on the material properties that are the most sensitive to manufacturing processes such as the BH curve and the specific core losses

The key observations from this work can be summarized as:

- 1) There are negligible variations on the machine performance when a design based on the properties of DS1 is compared to a design based on DS2. This is as expected as in reality the processes used for DS1 and DS2 are basically the same with the only difference being that the DS2 data was produced in house.
- 2) There are significant variations in the machine performance when the machine design is performed using the data in DS3, i.e. when the material data does consider the manufacturing processes required to produce a stator stack. These can be categorized as follows
  - a. A drastic increase in specific core loss.
    - i. In general, the core losses increase drastically across the full operating range which results in lower efficiencies of the designed machine when considering data from DS3.
    - ii. In particular, a 23.5% increase in the stator core loss was observed at the rated operating point of 8700rpm, relative to when the information from DS1 and DS2 is used.
    - iii. A 16.7% increase in stator core loss was observed at the maximum operational speed of 19000rpm.
 

The above are mainly due to the lower flux density in both the teeth and the back iron (flux weakening region).
  - b. A significant reduction in magnetic field strength.
    - i. It’s observed that at lower magnetic field strength the reduction in the flux density was significant and this variation tend to decrease towards the saturation region. This reduction in the magnetic flux density results in a lower output torque of the designed machine.
    - ii. For such a machine, the reduction in the output torque at full load condition was 0.8%. While, small effect was noted beyond the base speed due to the increase in the negative d-axis current and therefore small variation in the flux density.
  - c. Reduced efficiency performances
    - i. An overall reduction in machine efficiency of 1% was observed when the data from DS3 was considered and compared to the designs that utilized data from DS1 and DS2. This variation is related to the reduction in the output torque and the increased core loss, highlighted in the above points a) and b).
    - ii. For this particular application, where the highest speed is 19000rpm, a 1% efficiency reduction is not considered to be a major issue. However, it is important to note that for higher speed applications, this can and will have a much more negative impact.



This work has thus indicated and confirmed that the often-overlooked effects of manufacturing processes can have a significant and important effect on the overall machine performance. While in the particular case considered here the described effects were not of particularly high values, however it is clear that in the quest for higher performance and higher speed applications, then the above aspects need to be given careful attention.

As a final remark, it is worth noting that for the PMSM of this case study, the main resulting consideration was the 1% reduction in the general efficiency. For a high performance aerospace application, a 1% efficiency reduction cannot be neglected and in fact for the particular application at hand, the problem was solved by using ultra-thin laminations at the cost of more expensive material and less mechanical strength.

### VIII. ACKNOWLEDGMENT

This work was supported by the Ningbo Science & Technology Beauru under Grant 2014A35007 and by the Ningbo Science & Technology Beauru under Grant 2017A610089.

### IX. REFERENCES

- [1] *Methods of Measurement of Magnetic Properties of Magnetic Sheet and Strip at Medium Frequencies*, Int. Std. IEC 60404-10:1988.
- [2] *Methods of Measurement of the Magnetic Properties of Electrical Steel Strip and Sheet by Means of an Epstein Frame*, Int. Std. IEC 60404-2:1996+A1:2008.
- [3] M. Cossale, A. Krings, J. Soulard, A. Boglietti and A. Cavagnino, "Practical Investigations on Cobalt-Iron Laminations for Electrical Machines," in *IEEE Transactions on Industry Applications*, vol. 51, no. 4, pp. 2933-2939, July-Aug. 2015.
- [4] Goes, P., E. Hoferlin, and M. De Wulf. "Calculating iron losses taking into account effects of manufacturing processes." *Proc. of COMSOL Conference*. 2008.
- [5] P. Giangrande, F. Cupertino and G. Pellegrino, "Modelling of linear motor end-effects for saliency based sensorless control", 2010 *IEEE Energy Conversion Congress and Exposition (ECCE)*, Atlanta, GA, USA, September 2010.
- [6] Z. Gmyrek, A. Cavagnino and L. Ferraris, "Estimation of the Magnetic Properties of the Damaged Area Resulting From the Punching Process: Experimental Research and FEM Modeling," in *IEEE Transactions on Industry Applications*, vol. 49, no. 5, pp. 2069-2077, Sept.-Oct. 2013.
- [7] M. S. Lim, J. H. Kim and J. P. Hong, "Experimental Characterization of the Slinky-Laminated Core and Iron Loss Analysis of Electrical Machine," in *IEEE Transactions on Magnetics*, vol. 51, no. 11, pp. 1-4, Nov. 2015.
- [8] S. Elfgen, S. Steentjes, S. Böhmer, D. Franck and K. Hameyer, "Influences of Material Degradation Due to Laser Cutting on the Operating Behavior of PMSM Using a Continuous Local Material Model," in *IEEE Transactions on Industry Applications*, vol. 53, no. 3, pp. 1978-1984, May-June 2017.
- [9] N. Fernando, G. Vakil, P. Arumugam, E. Amankwah, C. Gerada and S. Bozhko, "Impact of Soft Magnetic Material on Design of High-Speed Permanent-Magnet Machines," in *IEEE Transactions on Industrial Electronics*, vol. 64, no. 3, pp. 2415-2423, March 2017.
- [10] M. Dems and K. Komez, "The Influence of Electrical Sheet on the Core Losses at No-Load and Full-Load of Small Power Induction Motors," in *IEEE Transactions on Industrial Electronics*, vol. 64, no. 3, pp. 2433-2442, March 2017.
- [11] M. Dems and K. Komez, "Performance Characteristics of a High-Speed Energy-Saving Induction Motor With an Amorphous Stator Core," in *IEEE Transactions on Industrial Electronics*, vol. 61, no. 6, pp. 3046-3055, June 2014.
- [12] D. G. Ahn, M. H. Yoon, S. I. Kim and J. P. Hong, "Welding loss modeling and evaluation of electric motors using laminated cores," 2016 *IEEE Conference on Electromagnetic Field Computation (CEFC)*, Miami, FL, 2016, pp. 1-1.
- [13] A. Krings, S. Nategh, O. Wallmark and J. Soulard, "Influence of the Welding Process on the Performance of Slotless PM Motors With SiFe

- and NiFe Stator Laminations," in *IEEE Transactions on Industry Applications*, vol. 50, no. 1, pp. 296-306, Jan.-Feb. 2014.
- [14] A. Krings, S. Nategh, A. Stening, H. Grop, O. Wallmark, J. Soulard, "Measurement and modeling of iron losses in electrical machines." *5th International Conference Magnetism and Metallurgy WMM'12, June 20th to 22nd, 2012, Ghent, Belgium*. Gent University, 2012.
- [15] M. Galea, C. Gerada, T. Raminosa, and P. Wheeler, "A Thermal Improvement Technique for the Phase Windings of Electrical Machines," *Industry Applications, IEEE Transactions on*, vol. 48, issue 1, pp. 79-87, 2012.
- [16] M. Galea, C. Gerada, T. Raminosa, and P. Wheeler, "Design of a high force density tubular permanent magnet motor," in *Electrical Machines (ICEM), 2010, XIX International Conference on*, 2010, pp. 1-6.
- [17] C. Sciascera, P. Giangrande, L. Papini, C. Gerada and M. Galea, "Analytical Thermal Model for Fast Stator Winding Temperature Prediction", in *IEEE Transactions on Industrial Electronics*, vol. 64, n. 8, pp. 6116-6126, March 2017.
- [18] A. Al-Timimy, M. Degano, P. Giangrande, G. Lo Calzo, Z. Xu, M. Galea, C. Gerada, He. Zhang, L. Xia, "Design and optimization of a high power density machine for flooded industrial pump," 2016 *XXII International Conference on Electrical Machines (ICEM)*, Lausanne, 2016, pp. 1480-1
- [19] A. Al-Timimy, M. Degano, Z. Xu, G. Lo Calzo, P. Giangrande, M. Galea, C. Gerada, He Zhang, L. Xia, "Trade-off analysis and design of a high power density PM machine for flooded industrial pump," *IECON 2016 - 42nd Annual Conference of the IEEE Industrial Electronics Society*, Florence, 2016, pp. 1749-1754.
- [20] Z. Xu, A. Al-Timimy, M. Degano, P. Giangrande, G. Lo Calzo, H. Zhang, M. Galea, C. Gerada, S. Pickering, L. Xia, "Thermal management of a permanent magnet motor for a directly coupled pump," 2016 *XXII International Conference on Electrical Machines (ICEM)*, Lausanne, 2016, pp. 2738-2744.
- [21] A. Krings, A. Boglietti, A. Cavagnino and S. Sprague, "Soft Magnetic Material Status and Trends in Electric Machines," in *IEEE Transactions on Industrial Electronics*, vol. 64, no. 3, pp. 2405-2414, March 2017.
- [22] Volbers, Niklas, and Joachim Gerster. "High saturation high strength iron-cobalt alloy for electrical machines." *Proceedings of the INDUCTICA, CWIEME Berlin (2012)*.
- [23] A. Krings, M. Cossale, J. Soulard, A. Boglietti and A. Cavagnino, "Manufacturing influence on the magnetic properties and iron losses in cobalt-iron stator cores for electrical machines," 2014 *IEEE Energy Conversion Congress and Exposition (ECCE)*, Pittsburgh, PA, 2014, pp. 5595-5601.
- [24] A. Krings and J. Soulard, "Experimental characterization of magnetic materials for electrical machine applications," 2015 *IEEE Workshop on Electrical Machines Design, Control and Diagnosis (WEMDCD)*, Torino, 2015, pp. 85-89.
- [25] A. M. Mohammed, T. Cox, M. Galea, C. Gerada, "A New Method for determining the Magnetic Properties of Solid Materials employed in Unconventional Magnetic Circuits," in *IEEE Transactions on Industrial Electronics*, vol. PP, no.99, pp.1-1
- [26] Clerc, Alexander J., and Annette Muetze. "Measurement of stator core magnetic degradation during the manufacturing process." *IEEE transactions on industry applications* 48.4 (2012): 1344-1352.
- [27] Puvan Arumugam, Zeyuan Xu, Antonino La Rocca, Gaurang Vakil, Matthew Dickinson, Emmanuel Amankwah, Tahar Hamiti, Serhiy Bozhko, Chris Gerada, Stephen J. Pickering, "High-Speed Solid Rotor Permanent Magnet Machines: Concept and Design," in *IEEE Transactions on Transportation Electrification*, vol. 2, no. 3, pp. 391-400, Sept. 2016.
- [28] A. Saleem, N. Alatawneh, R. R. Chromik and D. A. Lowther, "Effect of Shear Cutting on Microstructure and Magnetic Properties of Non-Oriented Electrical Steel," in *IEEE Transactions on Magnetics*, vol. 52, no. 5, pp. 1-4, May 2016.



**Ahmed Al-Timimy** received his M.Sc. degree in Electrical Engineering from the University of Technology, Baghdad, Iraq in 2012. He is currently working towards his PhD in electro-magnetic modelling and electrical machine design within the Power Electronics, Machines and Control (PEMC) Group at The University of Nottingham, Nottingham, UK. His main research interests are design and analysis of high performance electrical machines for aerospace applications.



**Gaurang Vakil** (M'16) received Ph.D. from Power Electronics, Machines and Drives (PEMD) group at Indian Institute of Technology - Delhi (IITD) in variable speed generator design for renewable energy applications in 2016. He subsequently worked as a Research Associate with Power Electronics, Machines and Controls (PEMC) group at the University of Nottingham. In 2016 he was appointed as an assistant professor with electrical and electronics engineering department in University of

Nottingham. His main research interests include analytical modelling and design optimization of electrical machines, optimizing electric drive-train for pure electric and hybrid vehicles, high power density machines, magnetic material characterization and highperformance electrical machines for transport and renewable generation.



**Michele Degano** (M'15) received the Laurea degree in electrical engineering from the University of Trieste, Trieste, Italy, in 2011, and the Ph.D. degree in industrial engineering from the University of Padova, Padova, Italy, in 2015. During his doctoral studies, he cooperated with several local companies for the design of permanent-magnet machines. In 2015, he joined the Power Electronics, Machines and Control Group, The University of Nottingham, Nottingham, U.K., as a Research Fellow, where

he is currently an Assistant Professor teaching advanced courses on electrical machines. His main research interests include design and optimization of permanent-magnet machines, reluctance and permanent-magnet-assisted synchronous reluctance motors through genetic optimization techniques, for automotive and aerospace applications, ranging from small to large power.



**Paolo Giangrande** was born in Monopoli, Italy, in March 1982. He received his PhD in electrical engineering at the Technical University of Bari in 2011. During 2008 he was a Marie Curie Intra-European Fellow at the University of Malta. Since January 2012, he is Research Fellow at the University of Nottingham within the PEMC group. His research interests include sensorless control of AC electric drives and intelligent motion control, as well as design, modeling and parameters

identification of electrical machine for aerospace application.



**Chris Gerada** (M'05–SM'12) received the Ph.D. degree in numerical modelling of electrical machines from The University of Nottingham, Nottingham, U.K., in 2005. He was a Researcher with The University of Nottingham, working on high-performance electrical drives and on the design and modelling of electromagnetic actuators for aerospace applications. Since 2006, he has been the Project Manager of the GE Aviation Strategic Partnership. In 2008, he became a Lecturer in electrical machines, in 2011, as an

Associate Professor, and in 2013, a Professor at The University of Nottingham. His main research interests include the design and modelling of high-performance electric drives and machines. Prof. Gerada serves as an Associate Editor for the IEEE TRANSACTIONS ON INDUSTRY APPLICATIONS and is the Chair of the IEEE Industrial Electronics Society Electrical Machines Committee.



**Michael Galea** (M'13) received his PhD in electrical machines design from the University of Nottingham, UK, where he has also worked as a Research Fellow. He is currently the Head of the School of Aerospace in the University of Nottingham, Ningbo, China, where he is also the Director of Aerospace. He is also the Deputy Director of the Institute for Aerospace Technology in the University of Nottingham, UK. He currently lectures in Electrical Drives and in Aerospace Systems Integration and manages a number of

diverse projects and programmes related to the more / all electric aircraft, electrified propulsion and associated fields. His main research interests are design, analysis and thermal management of electrical machines and drives, the more electric aircraft and electrified and hybrid propulsion.